SAND79-0514
Unlimited Release
UC-62

PERFORMANCE TESTING OF THE GENERAL ELECTRIC ENGINEERING PROTOTYPE COLLECTOR

Vernon E. Dudley, EG&G, Inc.
Robert M. Workhoven

Prepared by Sandia Laboratories, Albuquerque, New Mexico 87115 and Livermore, California 94550 for the United States Department of Energy under Contract AC04-76DP00789.

Printed July 1979

Sandia Laboratories

2900 Q(7-73)

Issued by Sandia Laboratories, operated for the United States Department of Energy by Sandia Corporation.

NOTICE

Printed in the United States of America

Available from
National Technical Information Service
U. S. Department of Commerce
5285 Port Royal Road
Springfield, VA 22161

Price: Printed Copy $4.50 ; Microfiche $3.00

SAND79-0514
Unlimited Release
Printed July 1979

Performance Testing of the General Electric Engineering Prototype Collector

Vernon E. Dudley
Energy Measurements Group
EG&G, Inc.

Robert M. Workhoven
Experimental Systems Operations Division 4721
Sandia Laboratories
Albuquerque, NM 87185

ABSTRACT

This report provides results of tests on the General Electric Engineering Prototype Collector, a 5-meter parabolic dish solar concentrator.

CONTENTS

ILLUSTRATIONS

TABLES

PERFORMANCE TESTING OF THE GENERAL ELECTRIC ENGINEERING PROTOTYPE COLLECTOR

Introduction

A series of concentrating solar collector designs is being tested at the Sandia Laboratories Collector Module Test Facility (CMTF). This facility operates as part of the Department of Energy's continuing program to characterize selected collector modules for possible future systems use.[1] Several of the collector designs tested have been chosen to provide the energy input for solar-powered demonstration projects. The GE parabolic dish collector evaluated for this report is a first prototype for a solar total energy system proposed for a knitwear plant at Shenandoah, Georgia.

Test Objective

One planned objective of the Department of Energy's Solar Thermal Power Systems program is the establishment of a large scale solar total energy system at an operating industrial plant. As part of the systems study for such a large-scale solar total energy experiment, General Electric has constructed a first prototype of a large parabolic dish solar collector. Short time scales prevented the design of a parabolic dish mirror custom tailored to the requirements of the solar system, so a dish originally designed for use as a communications antenna reflector was used.

The objective of this test series was to characterize the performance of the General Electric Engineering Prototype Collector (EPC). Items of particular interest were the thermal efficiency and thermal losses at temperatures from $\sim 100^{\circ}C$ to $\sim 300^{\circ}C$. Although the operational version of the prototype collector will operate at higher temperatures, the maximum test temperature at the CMTF is currently limited to about $315^{\circ}C$.

Collector Description

The parabolic dish used in the GE prototype collector was originally designed as a communications antenna reflector by Scientific-Atlanta, Inc. It was assembled at the Sandia test site by Scientific-Atlanta personnel. Figure 1 is a photograph of the collector after installation at the CMTF.

The collector dish constructed is 5 meters in diameter, and is made up of 24 sections of stamped aluminum sheet. The 15° arc segment dish sections are bolted together along flanges on the back side of each joint. The reflecting surface is covered with FEK-244, a second-surface aluminized acrylic film manufactured by the 3M company.

Trade-off studies indicated that a focal length to diameter ratio of about 0.5 would be an optimum value for the large scale experiment at Shenandoah. This ratio results in a required diameter of 3.75 meters for the reflector used at Sandia for this test. The effective diameter of the dish was therefore reduced from 5 meters to 3.75 meters by painting a ring 0.625 meters wide around the outer edge of the dish. Any final design would not include such a feature; the procedure was adopted in the interest of gathering some test data on a prototype in minimum time.

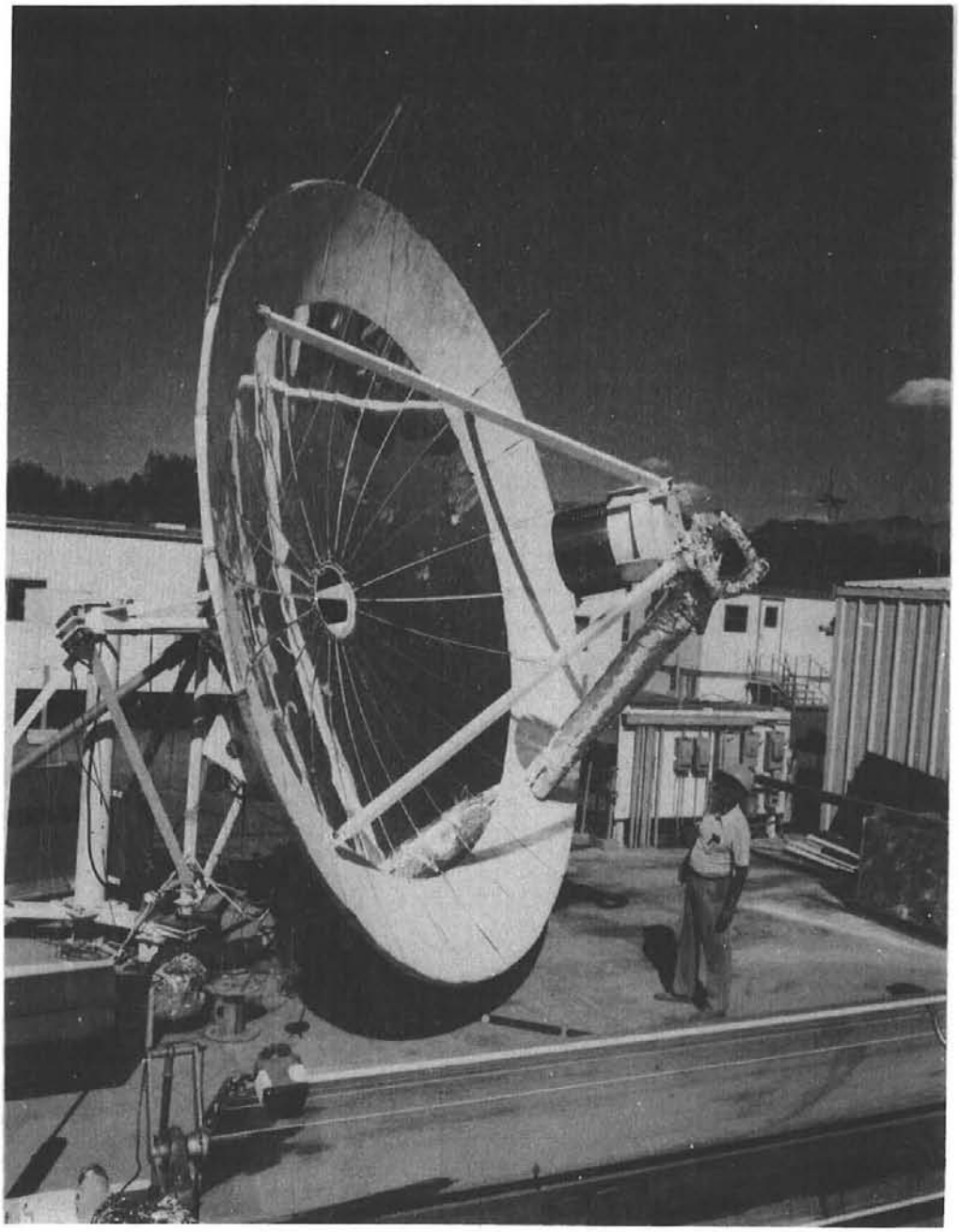

Figure 1. GE EPC Parabolic Dish.

The GE receiver installed on the dish was an insulated cylindrical cavity; aperture plates of several sizes were used on the mouth of the cavity. Coiled around the inner walls of the receiver cavity was 26.2 meters of stainless steel absorber tubing. Figure 2 shows a cross-sectional view of the receiver. The absorber tubing was 11.11 mm in diameter, and had been oxidized by heating to about 1100°C, resulting in a surface absorptivity of about 0.88.

The collector dish and receiver were supported by a structure of steel channel, angle, and tubing. Electric-motor-driven jackscrews were used to drive the collector for azimuth and elevation positioning. Since this prototype collector did not have to cover the range of sun positions expected of an operational system, the support and drive systems were simplified by restricting the azimuth coverage to a range from 18° north of east to 10° west of south. Similarly, the elevation angle coverage was restricted to angles between 15° and 80° above the horizontal.

Sun tracking and positioning of the collector were available in four modes: (1) a computer system (2) a sun sensor (3) a combined sun sensor/computer and (4) manual control.

In the computer track mode, a Sandia-furnished HP 9825 computer calculated sun azimuth and sun elevation angles. These angles were compared to actual collector position to derive an error signal to drive the collector to the proper position.

Using the sun-sensor tracking mode, a solid-state logic and control package manufactured by Mann-Russell was used with a sun sensor to provide direct sun tracking. The electronics package also included a timer that could provide approximate position data when the sun was obscured by cloud cover. In the final design, the sun sensor will monitor reflected light at the receiver aperture. For this experiment, the sun sensor was mounted on the rim of the dish and monitored direct solar radiation.

A combined computer/sun sensor mode provided tracking under computer control until the position error in each axis dropped below 1/2 degree. If the solar radiation input was also above a preset threshold, the system then switched to the sun sensor for direct tracking. If the insolation level subsequently dropped below the selected threshold, tracking reverted to computer control. This system provided the fine tracking resolution available from the narrow angle sun sensor in bright sunlight, while the threshold level and computer prevented the sun sensor system from tracking bright edges of clouds during less ideal sky conditions.

GE instrumented the receiver with 22 chromel-constantan thermocouples welded to the absorber tube coils. Thirty additional chromel-constantan thermocouples were located on the receiver housing. In addition to the above receiver instrumentation, copper-constantan thermocouples were installed in the fluid input and output lines by Sandia.

Test Facility Description

The CMTF's fluid Loop 1 is designed to supply Therminol-66 as a heat-transfer fluid at temperatures from about 100 to 300°C. Characteristics of Therminol-66 are given in Reference 2. Design flow rates available from Loop 1 range from 4 L/min to 40 L/min. For tests of the GE EPC, maximum flow rates were about 8 L/min.

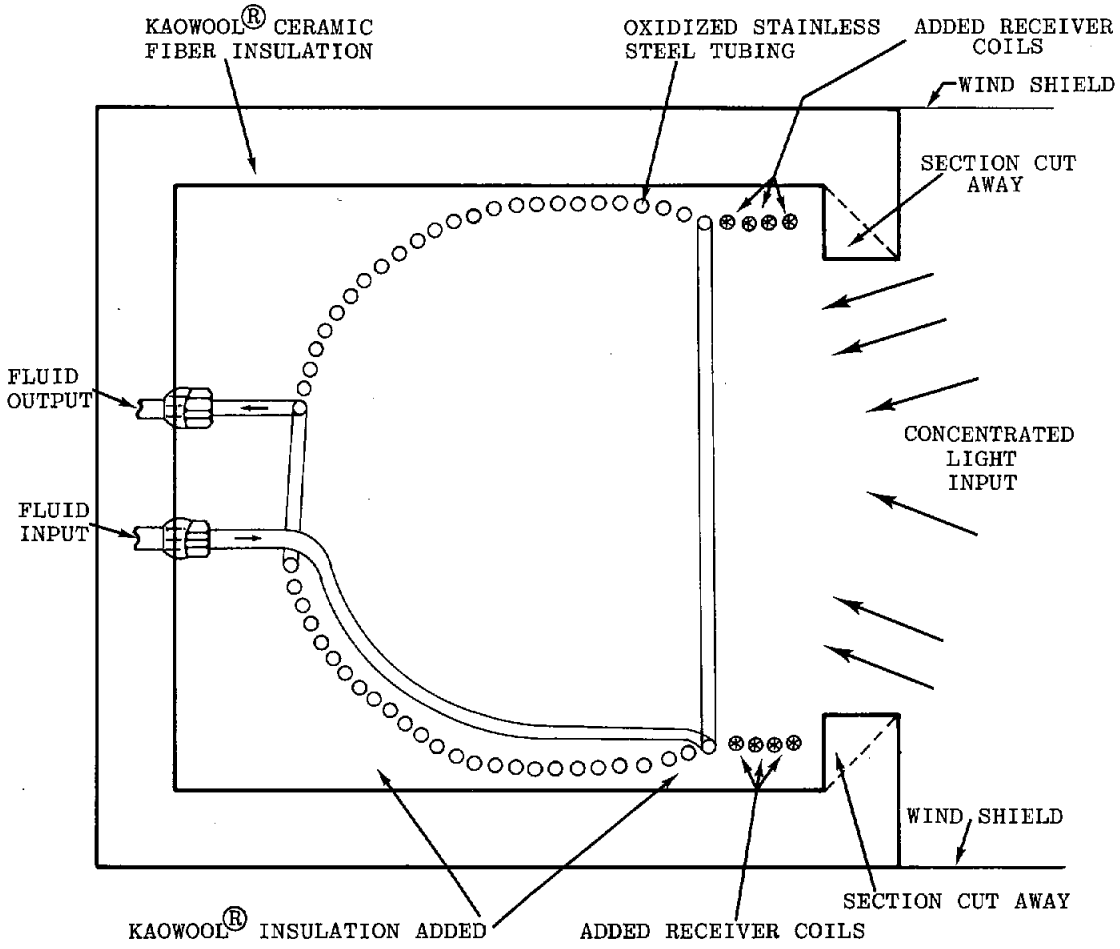

Figure 2. GE EPC Receiver Cross Section

A typical test day began by heating the fluid loop with electric heaters; the collector dish was placed in focus as soon as an appropriate fluid flow was established. An additional parabolic trough collector system was often used in parallel with the GE EPC to speed heating of the fluid system to the desired operating temperature. Data collection was usually attempted at only one operating temperature in one day because of the time required for temperature stabilization. During an individual test both the input temperature and fluid flow rate were maintained constant while the output temperature varied according to the test conditions.

Fluid flow-rate was measured with a turbine flowmeter manufactured by Flow Technology, Inc. Two flowmeters in series were used on several occasions as a cross-check on flowmeter accuracy. Prior to the test series, and several times during the tests, the flowmeter was calibrated by flowing fluid into a container. The fluid container weight vs.time was measured to determine the true flow-rate.

Direct solar radiation measurement was provided by an Eppley pyrheliometer. Ambient temperature, wind speed and wind direction were also recorded.

The data from the instruments described above were converted to digital format by Doric 210 and 220 analog-to-digital data systems. An HP 2116 minicomputer processed the input data and a printed sheet of the critical data for the test being performed was provided as output.

Figures 3 and 4 contain reproductions of the printed output for an efficiency test and for a thermal loss test, respectively. Unless otherwise labeled, the temperatures listed are in degrees Celsius. The delta temperature listed is not the arithmetic difference of the input and output temperatures, but was calculated from the differential output of the in-out thermocouples.

The speed of the data system was such that all of the data channels could be read, the calculations could be performed, and a line in the data table printed in about 20 seconds. Thirty-one measured and calculated data values from the data system were recorded on magnetic tape every 20 seconds. Only those shown in Figures 3 and 4 were printed in real time. The average values were automatically printed after 10 data points were accumulated. The complete data printout (as shown in Figures 3 and 4) was repeated at intervals of about 3 minutes throughout a test run. The number of decimal places printed should not be taken as indicating the data system accuracy since the choice of the print format was dictated by the peculiarities of the computer system. Either a loss or an efficiency data print was made continuously when the system was operating; however, only those data blocks occurring under stable conditions are included in this report.

Performance Test Definitions

During a test run both the specific heat and density of the Therminol-66 were calculated for each data set using the average temperature of the fluid in the absorber tube and the properties of Therminol-66.[2] Heat gain (or loss) was then calculated by using the following formula:

$$Q = \dot{m} C_p \Delta T$$

in which

Q = heat gain, kJ/h
$\dot{m}$ = mass flow-rate of fluid, kg/h
C_p = specific heat of fluid, J/kg^{o}C
ΔT = in-out temperature differential, ^{o}C

♦♦♦♦♦ GE PARABOLIC DISH EFFICIENCY TEST ♦♦♦♦♦

TEST DATE: DECEMBER 4 1978 HOUR 11 MINUTE 35 (SOLAR TIME)

2.78	(DEG C)	AMBIENT TEMPERATURE	(DEG F) 37
14	WIND DIRECTION, DEGREES		
5.6	(M/SEC)	WIND SPEED	(MPH) 12.6

TEMP IN	TEMP OUT	SOLAR WATTS/M^2	DELTA TEMP	FLOW LITERS/MIN	EFFICIENCY PERCENT
224.94	248.89	1017	24.12	7.22	52.5
224.94	248.83	1019	24.14	7.21	52.4
224.94	248.83	1019.7	24.1	7.21	52.2
225	248.89	1018.2	24.14	7.22	52.5
225	248.89	1018.3	24.12	7.21	52.4
225	248.94	1018.8	24.12	7.21	52.3
225	248.83	1020.3	24.1	7.21	52.2
224.94	248.89	1020.3	24.14	7.21	52.3
224.94	248.83	1019.7	24.12	7.22	52.4
224.94	248.89	1019.3	24.3	7.19	52.5
	10 POINT AVERAGES				
224.964	248.871	1019.06	24.14	7.211	52.37

51.86	AVG EFFICIENCY USING SUB. DELTA T
21114.7	AVG HEAT GAIN (KJ/HR) (W/M^2)= 533.728
233.896	AVG RECVR TEMP MINUS AMB TEMP
.229521	(AVG TEMP-AMB T)/I
21917.1	REYNOLDS NUMBER

END OF DATA PASS 8

Figure 3. Sample of Efficiency Test Data Printout

♦♦♦♦♦ GE PARABOLIC DISH THERMAL LOSS TEST ♦♦♦♦♦

TEST DATE: DECEMBER 4 1978 HOUR 14 MINUTE 59 (SOLAR TIME)

5.44	(DEG C)	AMBIENT TEMPERATURE	(DEG F) 41.8
337	WIND DIRECTION, DEGREES		
5.8	(M/SEC)	WIND SPEED	(MPH) 13.1

TEMP IN	TEMP OUT	FLOW LITERS/MIN	DELTA TEMP	WATTS GAIN/LOSS
211.94	208.83	6.99	-2.94	-671.3
211.94	208.94	6.99	-2.88	-657.7
211.94	208.89	6.98	-2.87	-654.3
211.89	208.89	6.98	-2.87	-654.4
211.94	208.89	6.99	-2.88	-657.6
211.94	208.89	6.97	-2.81	-639.9
211.89	208.94	6.98	-2.79	-636.2
211.94	208.94	6.99	-2.81	-641.7
211.89	208.89	6.99	-2.88	-657.6
211.89	208.94	6.99	-2.79	-637.1
	10 POINT AVERAGES			
211.92	208.904	6.985	-2.852	-650.763

AVERAGE INSOLATION = 896.58 WATTS/M^2
AVG LOSS USING SUB. DELTA T (WATTS) = -688.18
AVG LOSSES: (KJ/HR)=-2342.56 (W/M^2)=-59.2141
AVG RECVR TEMP MINUS AMB TEMP 204.835
AVG REYNOLDS NUMBER 17330.2

END OF DATA PASS 3

Figure 4. Sample of Thermal Loss Data Printout

A successful loss measurement is defined as at least one 10-point data block during which the values for input and output temperatures remained constant to within $0.1^{o}C$ or less, the flow-rate varied by 0.1 L/min or less and the delta temperature changed by $0.1^{o}C$ or less.

Most loss test data points reported are averages of several 10-point data blocks, each block judged stable as described above, and with conditions nearly constant over the entire time averaged. Loss tests were conducted with the collector system near its normal operating position, but sufficiently defocused so that no light from the mirror would strike any part of the receiver assembly.

On most days, efficiency measurements were made until the collector reached its maximum westward azimuth, approximately 30 minutes after noon. Loss measurements were made for about two hours after completion of efficiency tests; the fluid loop was then placed in a cooling mode prior to shutdown for the day.

For an efficiency test, efficiency was calculated from the following formula:

$$\eta = \frac{Q/A}{I}$$

in which

η = solar collector efficiency
Q = heat gain, W
A = Collector aperture area, m^2
I = direct solar radiation, W/m^2

A successful efficiency data point measurement consists of at least one of the 10 point averages during which input and output temperatures changed by $0.1^{o}C$ or less, the flow rates varied by 0.1 L/min or less, the delta temperatures remained within $0.1^{o}C$ or less, and solar radiation remained constant to about 1%. Temperatures, flow-rate, and insolation had to have been nearly as stable as described above for at least five to ten minutes prior to the measurement; otherwise that data point was not considered to be a reliable measurement. Efficiency measurements are normally made with direct solar radiation greater than about 900 W/m^2.

The temperature, flow-rate and solar radiation stability criteria outlined above are necessary because the heat gain formula given assumes steady-state conditions. If near steady-state conditions can be achieved during a collector test, the computed values for heat gain (or loss) and efficiency will be nearly constant also, with some scatter in the data due to noise. Because of the thermal mass of the collector system, any change in temperature, flow-rate or insolation will result in measurements that do not correctly represent the performance of the collector.

Even on a sunny day that appears ideal for testing a solar collector, there are still variations in solar radiation. However, these variations can be relatively small, as can be seen in several of the test data plots later in this report. Small, rapid variations of this kind produce scatter in the efficiency data, but no long-term systematic errors.

As operated at the CMTF, the heat-transfer fluid supply loop tends to produce fluid flow-rate variations similar to those seen in the solar radiation input--small, rapid fluctuations with no long-term trend towards a higher or lower rate. These variations also produce scatter in the measured data.

Small, rapid temperature fluctuations also appear in the measured data, again producing data scatter. However, the temperature measurements are subject to fairly long-term, slow changes that can result in fairly large, systematic errors in heat gain/loss and efficiency calculations. One typical source of this kind of temperature drift is the constantly increasing temperature that occurs each test day as the system is heated towards the intended operating temperature. Another is the temperature decay that continues for very long times after the collector system is defocused to begin a thermal loss test.

At the CMTF, collector input and output temperatures are usually measured less than one second apart in time. However, the fluid whose temperature is being measured at the collector input may not arrive at the collector output for a relatively long time--from several seconds up to several minutes. Thus an efficiency, or heat gain/loss, measurement will not be valid unless the input and output temperatures are stable for at least as long as the transit time of the heat-transfer fluid through the system.

Because of the thermal mass of both the fluid supply system and the collector, stable temperatures must be held for relatively long periods of time before the complete system is in thermal equilibrium and valid measurements can be made. A small constant drift in temperatures can produce test data that looks quite acceptable; however, it contains a systematic error because of the thermal mass shift of in-out delta temperature. With one collector tested, a constant temperature increase of $0.7^{\circ}C$ per minute produced an efficiency measurement that had a very small data scatter and had a nearly constant efficiency value for more than an hour. This measured efficiency value turned out to be 5 percentage points lower than the efficiency measured later with more stable temperatures.

In another case, with a collector system of greater thermal mass, a similar slow drift in input temperature produced an efficiency measurement 15 percentage points lower than the true value.

If the input temperature drift is towards lower temperatures, errors of similar magnitude result, but the measured efficiency will be greater than the value obtained under stable conditions.

The same problem as outlined above for an efficiency measurement also occurs during thermal loss measurements. The error in thermal loss from unstable temperatures is larger than the efficiency error because the receiver delta temperature during a loss test is usually much less than during an efficiency measurement.

The requirement for $0.1^{\circ}C$ stability in measured temperatures for a usable data point is empirically based. It appears to produce valid data, and is also about as good as the fluid loop and collector system can attain in the outdoor test environment.

Test Results

Initial test results from the GE EPC were disappointing, and the measured efficiency decreased rapidly with increasing temperatures. Figure 5 is a typical plot of solar radiation and efficiency data made during an efficiency test. These plots were made each day in real time, and have proven invaluable in detecting data trends and oscillations, such as those visible in Figure 5, that are not obvious from tabular printed output.

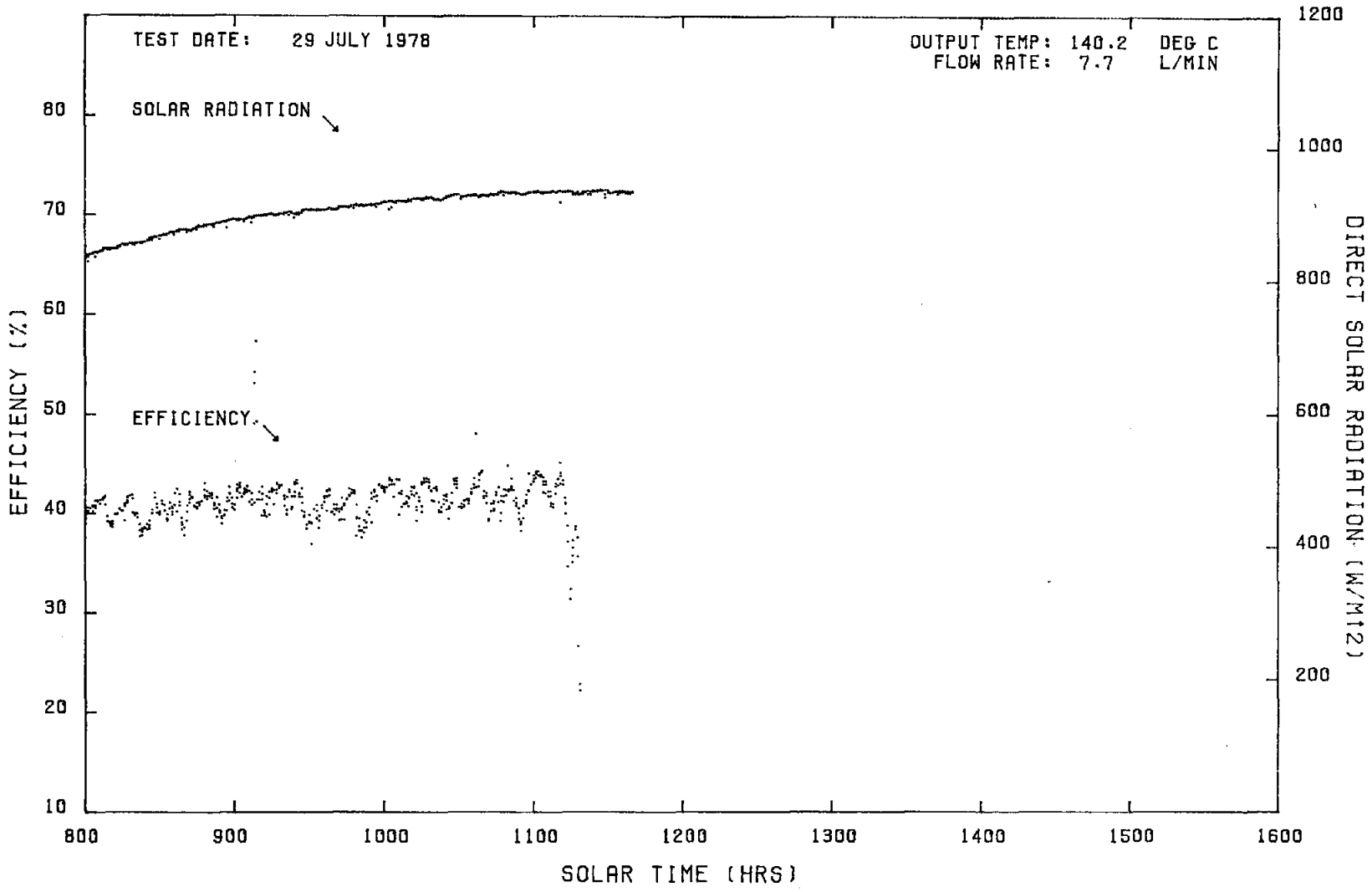

FIGURE 5 GE PARABOLIC DISH EFFICIENCY EVALUATION AT 121.2 DEG C INPUT

In Figure 5, the solar radiation input was quite stable, and greater than 800 W/m^2 even at 8:00 am. The measured efficiency was not very stable; the $\pm$2% oscillation was associated with sun tracking, but not directly due to "hunting" of the control system.

Each dot making up the curves in Figure 5 and subsequent real-time data plots is the result of a complete data collection cycle, repeating at about 20 second intervals. In most of these data plots, the flow rate, input and output temperatures noted are those at solar noon; however, for Figure 5, these values were taken at 11:00 am. The rapid drop in efficiency beginning at 11:10 occurred as the collector was defocused to begin thermal loss testing.

Figure 5 also illustrates another characteristic of two-axis tracking solar collectors: nearly constant efficiency throughout the day. This particular collector was not set up to track the sun after about 12:20 pm, otherwise, at a constant temperature the efficiency curve would be nearly a straight line for reasonably high solar radiation inputs.

Figure 6 was obtained at a higher operating temperature, and shows an attempt to determine the sensitivity of the receiver to different flow rates. In Figure 6, the efficiency points show a downward trend before 9:30 am, as the system was heated towards the desired 260°C. The efficiency rose again as the temperatures were stabilized at about 10:00 am. At about 10:10, the flow rate was changed from 8 L/min to 4 L/min. At 11:10 the flow was again cut in half, to 2 L/min. Any correlation between flow rate and efficiency appears to be less than the $\pm$2% oscillations occurring during this test. At 12:20 pm, the collector system reached its maximum westward azimuth and was defocused.

Figure 7 summarizes the first series of efficiency test results. Figure 8 shows the measured thermal losses. Except for the real-time data plots, the curves in all the figures in this report are the result of a least-squares fit to the test data.

Analysis of the collector hardware, efficiency data, and thermal loss data revealed several areas of possible improvement for the system: (1) the focal length of the dish was apparently slightly shorter than calculated; this resulted in concentrated light striking the back and upper walls of the receiver cavity in locations where there was no receiver coil, (2) concentrated light was striking the walls of the cylindrical entrance aperture of the receiver, (3) both conductive and convective thermal losses were higher than anticipated, when measured in the normal operating position, with differing aperture plate sizes and again with the receiver aperture covered and insulated.

In addition to the above problem areas, two others had been identified and corrected earlier. The original installation located several support strut attachments such that the dish tended to be distorted in shape at some elevation angles. Also, the original painted rim around the dish surface (necessary to reduce the effective diameter to the desired value) used black paint. Sunlight on the black surface heated this portion of the structure considerably more than the remainder of the active dish diameter, tending to distort the dish shape. Both these shape-distortion problems had been corrected prior to most of the data shown in Figure 5.

At this point, the receiver assembly was removed and returned to GE for an extensive laboratory test program to identify heat loss sources. To improve performance, a number of receiver modifications were made.

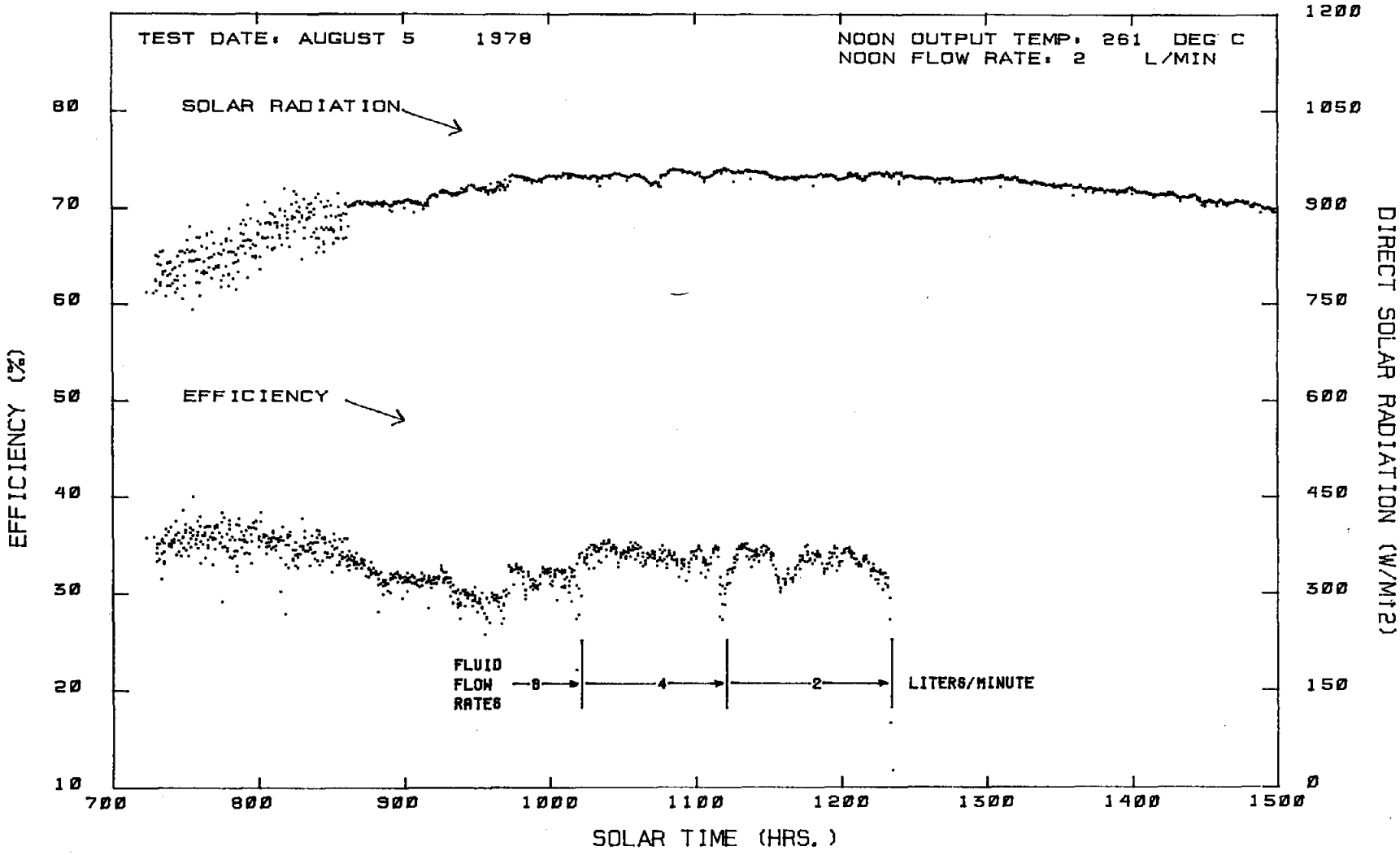

FIGURE 6 C E PARABOLIC DISH EFFICIENCY EVALUATION AT 204 DEG C INPUT

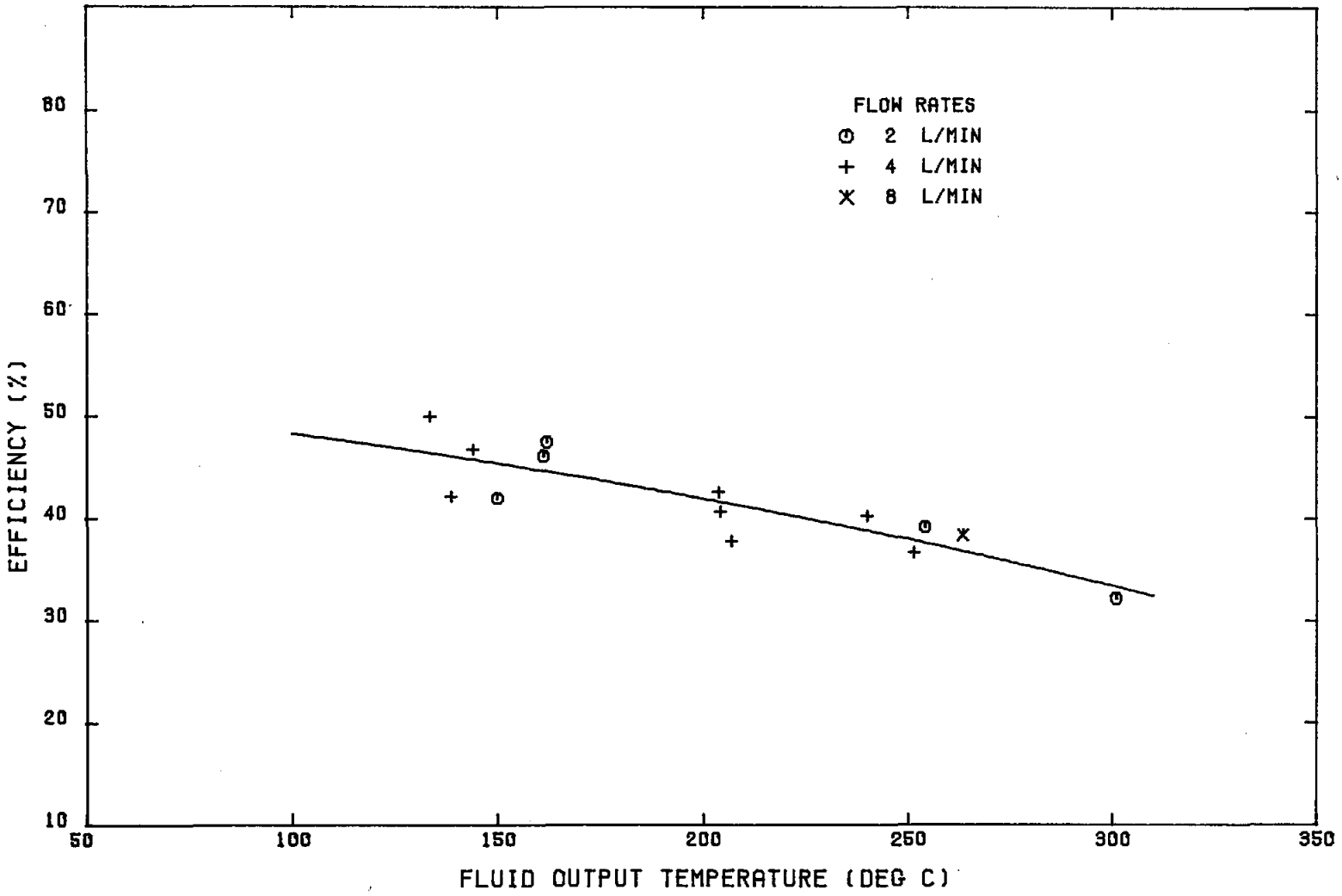

FIGURE 7 GE PARABOLIC DISH EFFICIENCY VS OUTPUT TEMPERATURE (ORIGINAL RECEIVER)

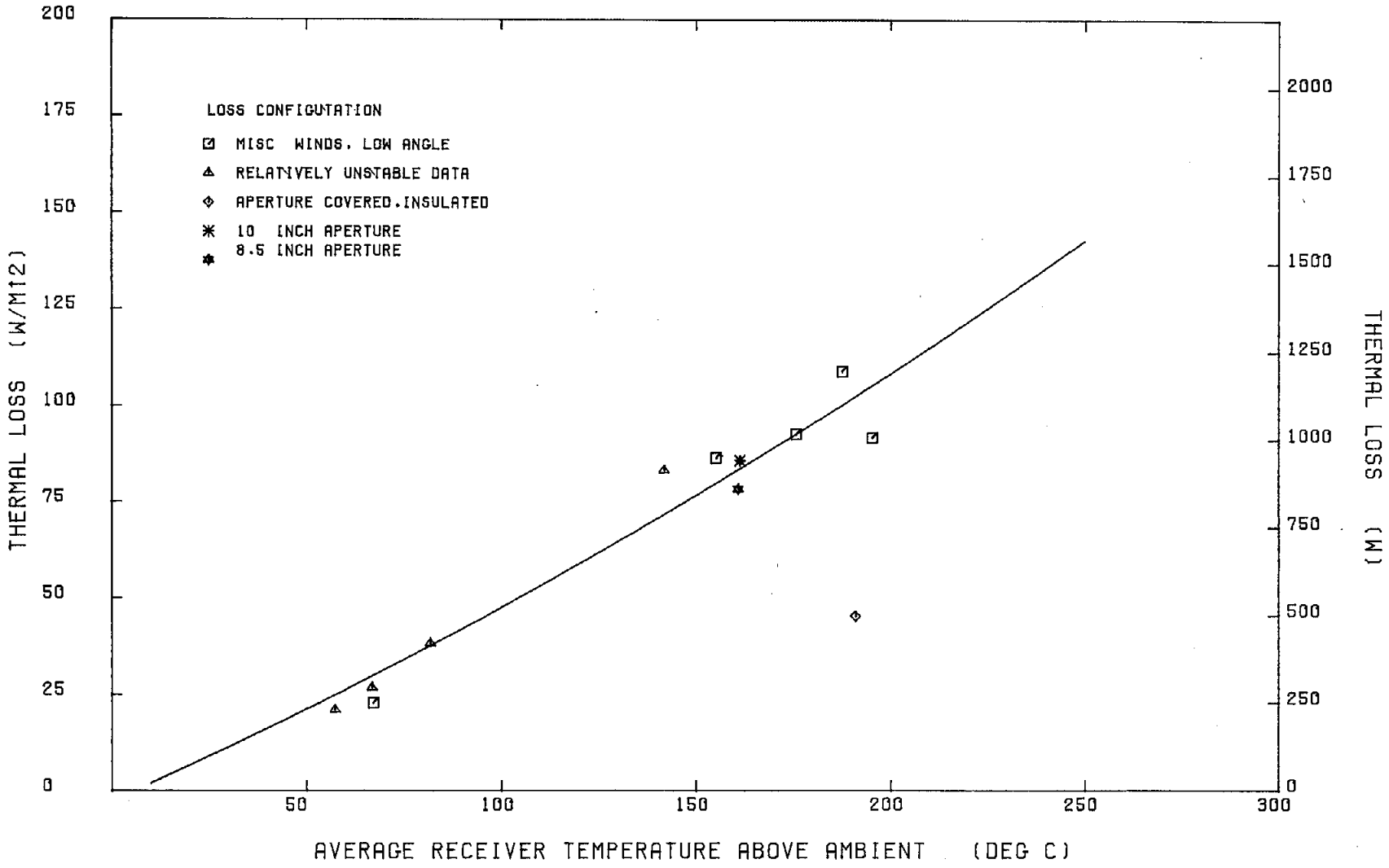

FIGURE 8 GE PARABOLIC DISH RECEIVER THERMAL LOSS (ORIGINAL RECEIVER)

The receiver assembly mounting brackets were changed so that the receiver could be moved closer to the dish surface, and thus into the correct focal position. The cylindrical entrance aperture was cut away to a sharp edge conical configuration, so that no light would be lost on the walls. Four coils of absorber tubing were added to the aperture end of the receiver cavity so that all the interior surface of the receiver cavity would be covered by an absorber surface. Finally, insulation was added between the absorber tubing and the receiver cavity walls and a cylindrical sleeve wind shield was added outside the receiver aperture to reduce convective heat losses. Two of these "fixes" are visible in Figure 1--the black ring around the dish was replaced by white paint, and the receiver wind shield is in place around the receiver aperture. The shield extends about 12 cm beyond the receiver aperture. The internal receiver modifications are called out in Figure 2.

When the modified receiver was reinstalled and testing resumed, the collector performance was drastically improved. Figure 9 is the result of an efficiency test on the redesigned receiver. The dish was placed in focus at 9:20 am; efficiency slowly increased as temperatures stabilized. The step in the curve at 10:50 am was caused by a change in input fluid temperature. At 12:26 pm, the output temperature was 190^{o}C, with a measured efficiency of 58.2%. At 12:33 pm, the dish mount reached its maximum westward travel. Note that the oscillations observed in the earlier tests have been largely eliminated.

Figure 10 illustrates a lower temperature test, at 168^{o}C output, during which the flow rate was changed from 7 L/min to 3 L/min, without any apparent effect on efficiency.

Figure 11 begins late in the morning because of the time required to clear the fluid lines of cold, congealed fluid and then heat the fluid system to high temperatures. As shown in the figure, the flow rates were decreased in steps from 8 L/min to 2 L/min. No decrease in efficiency is noticeable from 8 to 4 L/min, but a slow decrease of about 2% in measured efficiency occurred at 2 L/min. The decrease is slow, and the data more scattered at 2 L/min because of the long time required for the low flow rate to establish a new set of stable temperatures throughout the system. Finally, the efficiency decrease was checked by increasing the flow back to the original 8 L/min. The previously measured efficiency was quickly reestablished (within 1/2%) indicating a slight effect of flow rate on efficiency. Calculated Reynolds number at 8 L/min was 28,000 compared to 7,800 at 2 L/min.

Table 1 contains efficiency data from both receivers. Figure 12 shows the efficiency test results with the modified receiver, with efficiency shown as a function of output temperature. Figure 13 is the same test data presented as a function of average receiver temperature above ambient, divided by the input solar radiation.

Figure 14 shows a comparison of efficiency measured on the two receivers. The redesigned receiver improved the efficiency from ∿48% to ∿58% at 100^{o}C and from ∿33% to ∿54% at 300^{o}C.

Thermal loss from the redesigned GE receiver varied significantly with changes in wind velocity; these changes were less than those observed with the original receiver without the wind shield extension. For example, see the data in Table 2 for loss tests conducted November 2, 1978. The first point, showing 143 W loss, was taken with calm winds. The second data point was taken only 6 minutes later with variable, gusty winds of about 4-9 m/s; measured loss was now up to 250 W.

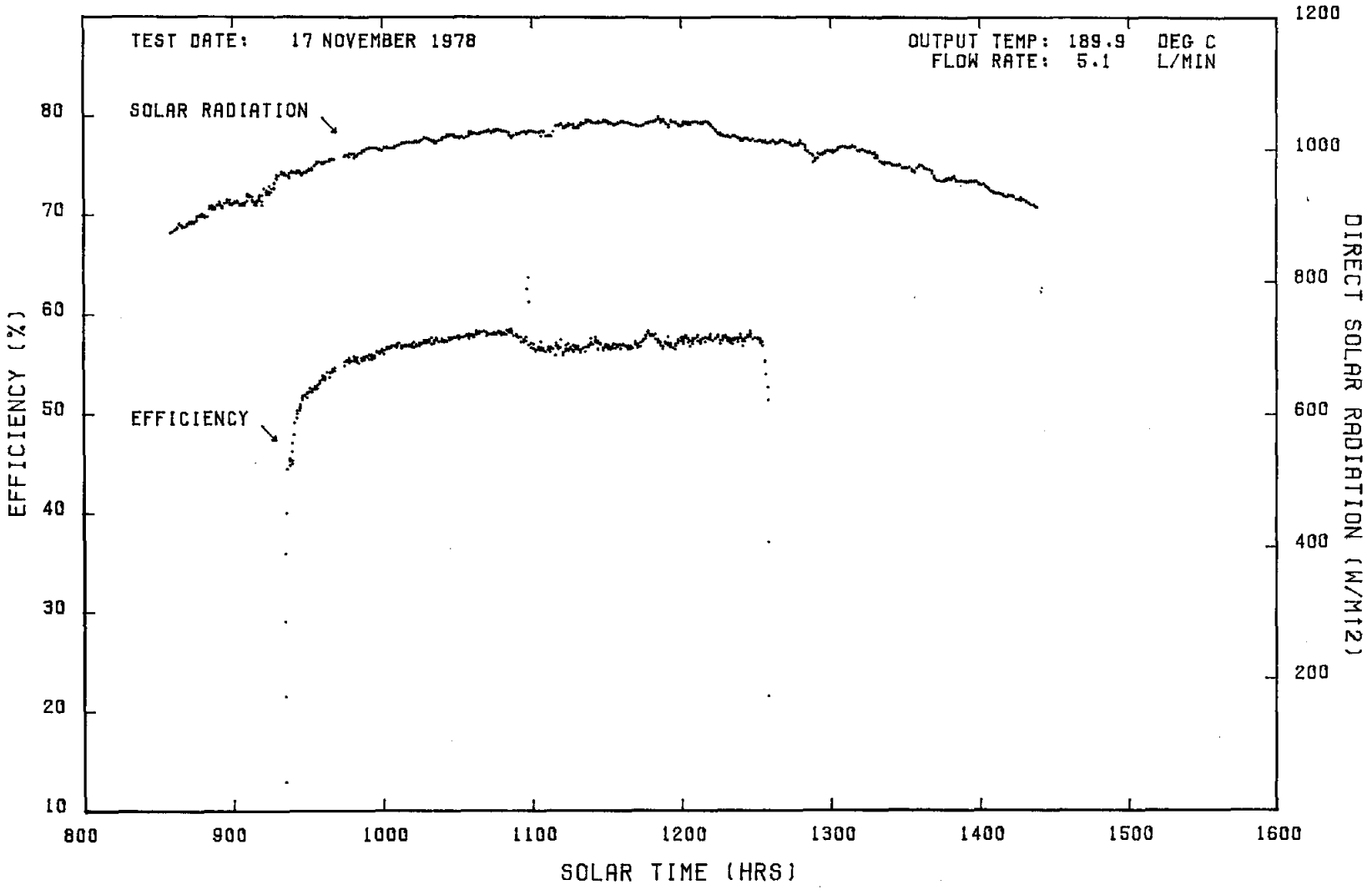

FIGURE 9 GE PARABOLIC DISH EFFICIENCY EVALUATION AT 150.1 DEG C INPUT

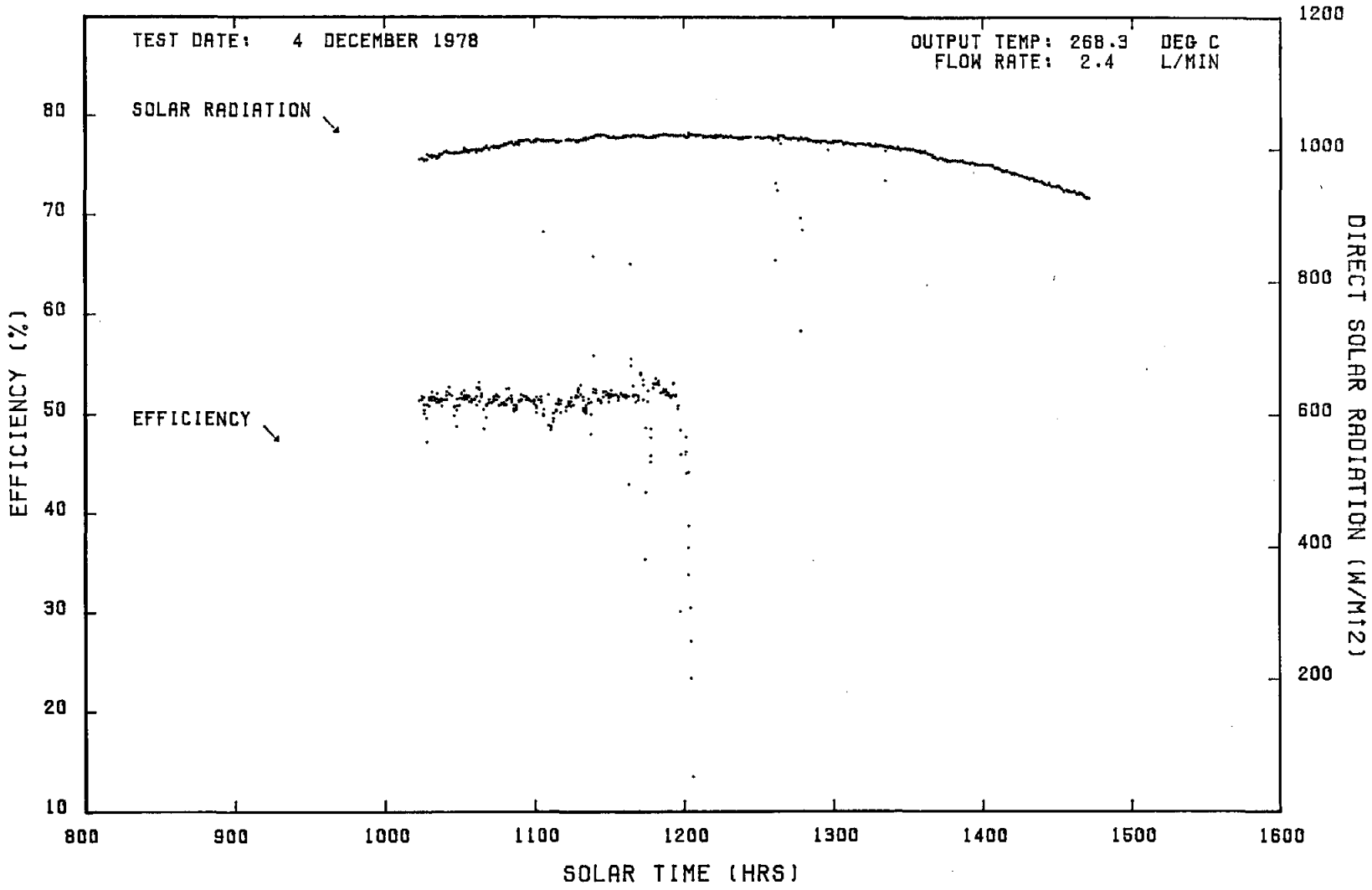

FIGURE 10 GE PARABOLIC DISH EFFICIENCY EVALUATION AT 214.7 DEG C INPUT

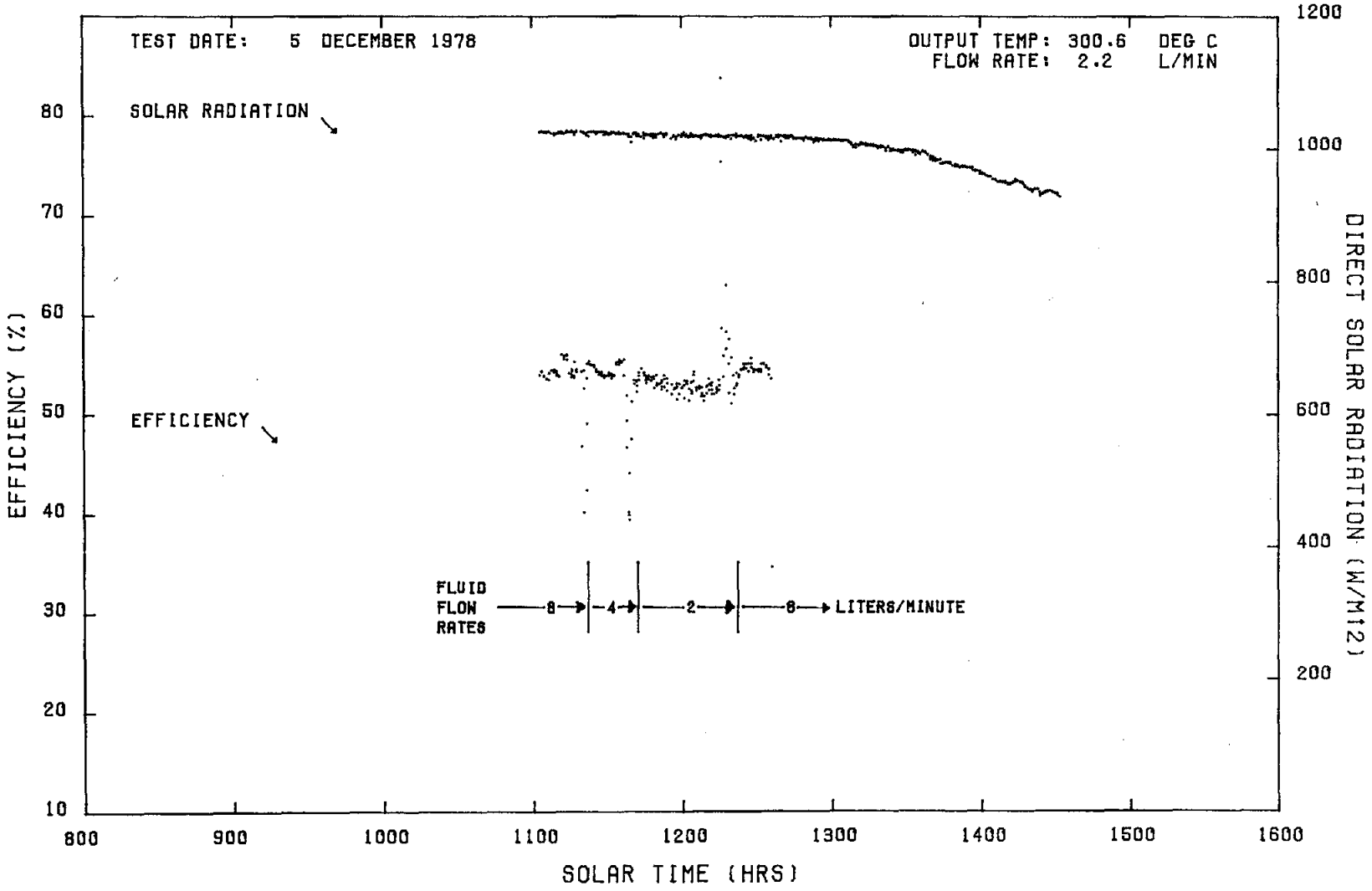

FIGURE 11 GE PARABOLIC DISH EFFICIENCY EVALUATION AT 223.0 DEG C INPUT

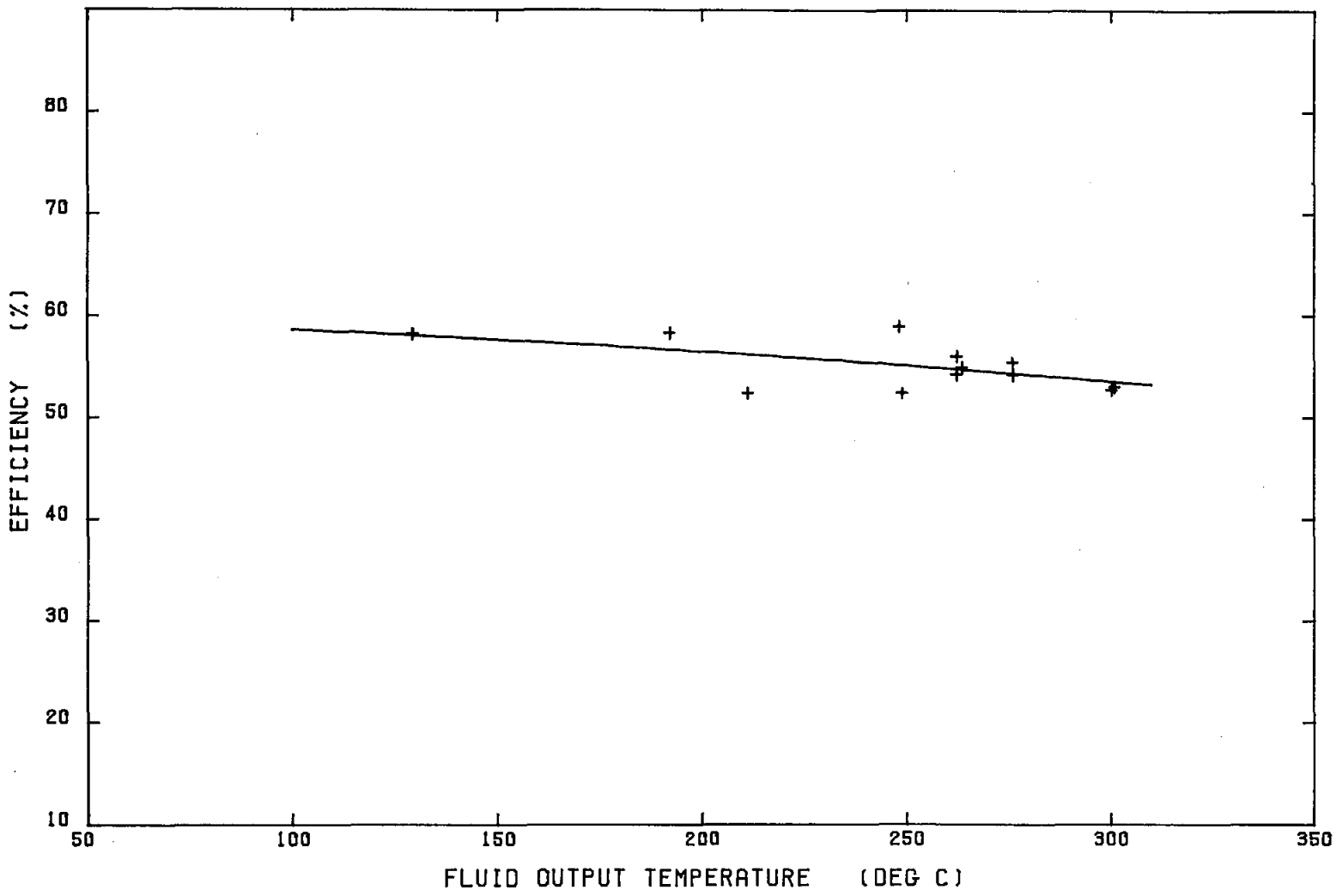

FIGURE 12 GE PARABOLIC DISH EFFICIENCY VS OUTPUT TEMPERATURE (REDESIGNED RECEIVER)

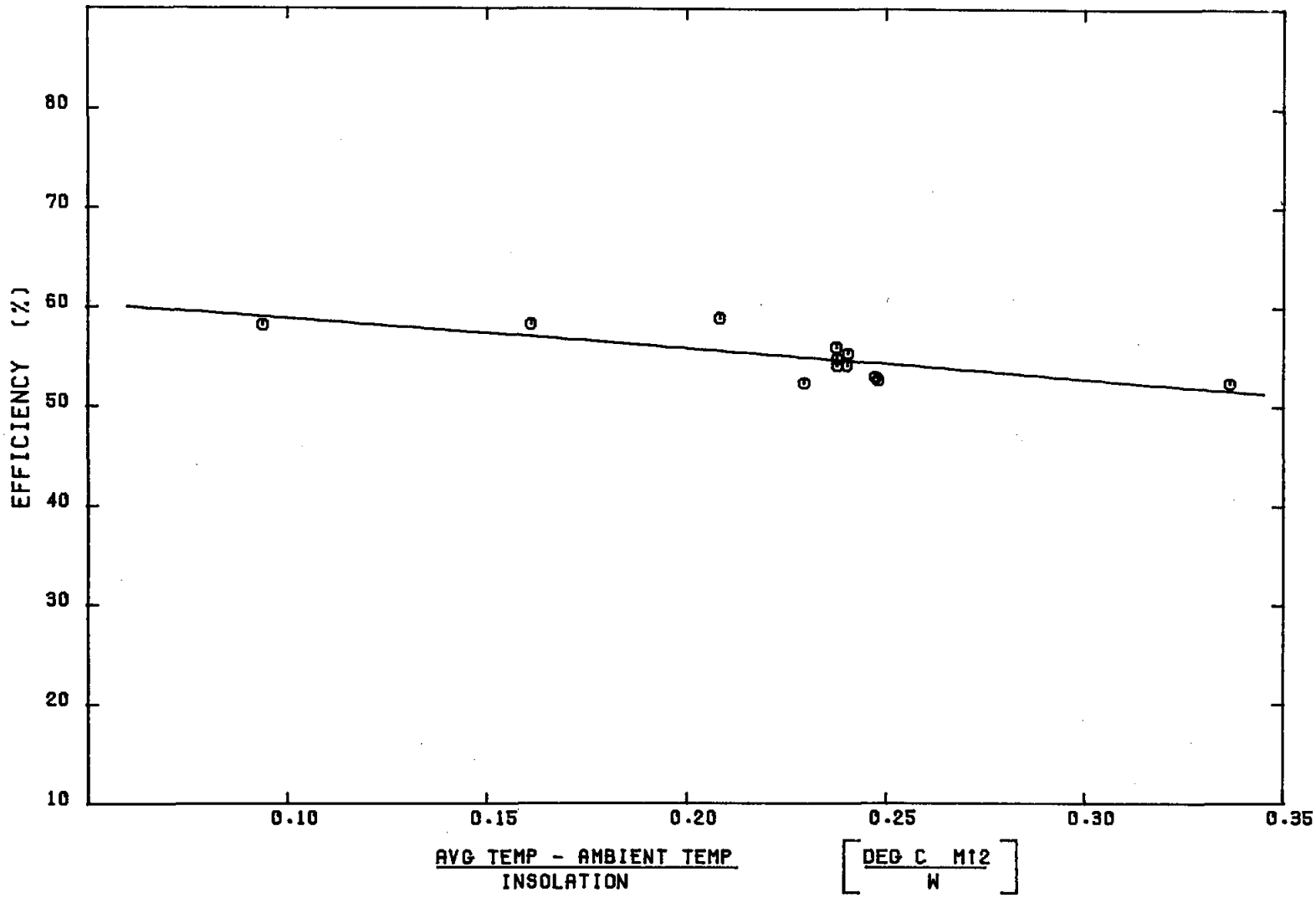

FIGURE 13 GE EPC EFFICIENCY VS DELTA TEMPERATURE/INSOLATION (REDESIGNED RECEIVER)

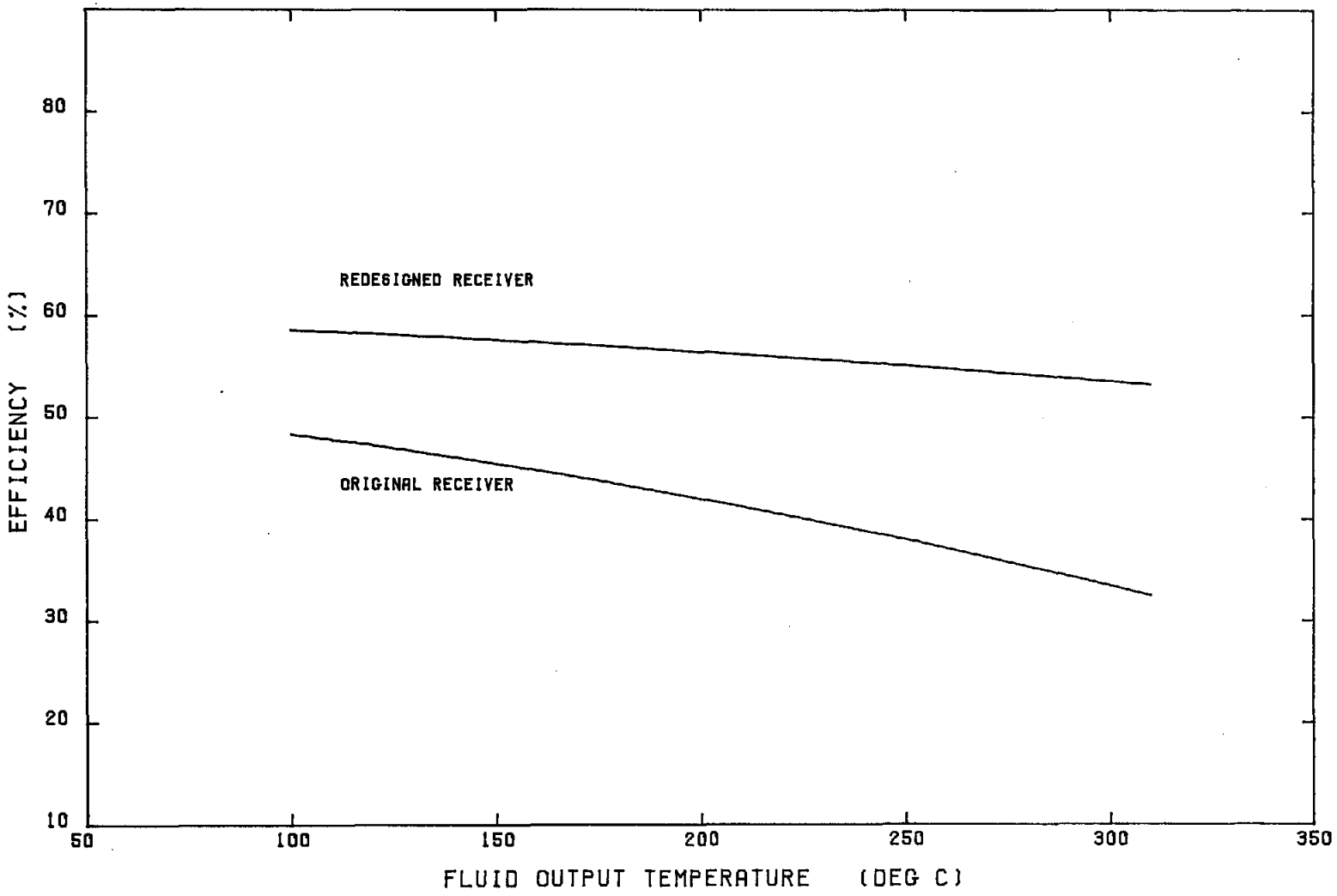

FIGURE 14 GE PARABOLIC DISH EFFICIENCY COMPARISON

Table 1

Efficiency Data for GE EPC

Test Date	Insolation (W/m^2)	Temperature Out (^oC)	Receiver Δ Temp (^oC)	Flow Rate (L/min)	Efficiency (%)
		Original Receiver			
7/7/78	978	161.2	42.6	3.75	46.1
7/7/78	982	162.0	43.4	3.81	47.5
7/7/78	983	144.0	22.0	7.47	46.8
7/29/78	890	150.0	32.3	4.13	42.0
7/29/78	915	138.7	18.1	7.66	42.2
7/31/78	955	204.3	16.4	7.97	40.7
8/1/78	936	133.5	22.1	7.65	50.0
8/2/78	911	240.1	15.1	7.96	40.3
8/3/78	856	203.8	15.2	8.07	42.6
8/5/78	950	251.4	14.2	7.98	36.7
8/5/78	953	254.3	31.7	3.85	39.2
8/5/78	950	263.4	58.3	2.05	38.4
8/8/78	956	300.9	25.7	3.79	32.2
8/9/78	917	206.8	13.9	8.36	37.8
		Redesigned Receiver			
11/17/78	1027	129.4	52.1	4.18	58.2
11/17/78	1016	192.2	39.4	5.13	58.3
11/18/78	1017	248.3	51.4	3.82	58.9
12/4/78	1019	248.9	24.1	7.21	52.4
12/5/78	1026	262.4	21.3	8.71	56.0
12/5/78	1024	275.9	42.5	4.3	55.4
12/5/78	1022	300.9	78.0	2.21	53.0
12/5/78	1020	263.5	22.6	7.99	54.9

Similar changes were noted on many occasions. Unfortunately, the wind flow around the receiver aperture changes drastically with wind direction because of the nearby dish. In the test installation this situation was further complicated by other collectors and two adjacent buildings. In addition, the wind measuring instruments were some distance away and at a different height. Therefore, a close correlation between wind velocity and thermal loss doesn't seem feasible using this set of test data. The test data was arbitrarily divided into two wind velocity groups; less than ∿2 m/s, and greater than ∿2 m/s. These two categories are plotted separately in Figure 10 as light winds and high winds.

Thermal loss was also observed to change with the elevation angle of the dish, apparently because convective air currents were greater at low elevation angles. For an example, see the three loss measurements made with similar wind conditions on November 17, 1978. The first measurement (206 watts) was made at about 45^o elevation. The second (157 watts) was measured at about $\sim 60^o$, and the third (339 watts) at $\sim 25^o$ elevation. This loss factor was observed on several occasions; not enough data is available at each elevation angle and wind condition to complete a definition of loss for each. Most of the Table 2 loss data was measured at

Table 2

Thermal Loss Data for GE EPC

Original Receiver

Test Date	Insolation (W/m^2)	Average Temp Above Ambient (°C)	Receiver ΔT (°C)	Flow Rate (L/min)	Wind (m/s)	Loss (W)	Note
6/2/78	850	81.8	3.84	3.67	9.4	420	
7/25/78	329	66.9	1.83	5.43	3.2	293	
7/25/78	930	57.4	4.79	1.65	3.5	231	
7/25/78	901	67.2	1.56	5.45	6.9	251	
7/31/78	959	155.2	3.66	8.01	5.2	949	
8/2/78	904	195.3	3.76	8.01	4.2	1007	
8/2/78	920	175.8	8.86	3.48	2.8	1018	
8/3/78	807	141.9	8.05	3.55	10.5	913	
8/4/78	80	193.1	5.46	7.81	10.3	1416	
8/5/78	921	187.6	8.59	4.20	6.4	1197	
8/5/78	897	191.0	3.58	4.18	4.8	498	1
8/9/78	915	161.4	3.61	8.02	1.5	941	2
8/9/78	905	161.0	3.30	8.02	8.6	860	3
		Redesigned Receiver					
10/26/78	910	162.2	2.25	3.26	--	227	
10/27/78	998	208.4	6.90	3.62	0.8	837	4
10/27/78	955	206.5	4.70	3.17	0.8	493	6
10/28/78	968	92.9	1.1	6.17	--	195	6
10/29/78	1024	210.9	2.4	8.46	--	682	6
10/29/78	1006	209.4	2.9	8.57	--	815	4
11/1/78	1.2	82.9	2.8	2.20	--	179	
11/2/78	429	84.7	1.3	3.86	<1	143	4
11/2/78	190	84.0	2.1	3.95	4.9	250	
11/2/78	762	83.9	1.4	3.96	<1	161	
11/2/78	516	83.6	1.98	3.96	∿6	233	6
11/3/78	1.2	154.8	4.96	3.54	∿7	557	
11/7/78	966	168.1	3.54	4.03	2.7	470	
11/8/78	982	202.8	4.47	3.33	0.4	503	4
11/9/78	946	117.1	1.84	3.59	1.0	202	
11/10/78	97	102.4	2.18	3.80	2.5	249	
11/13/78	852	98.9	1.91	3.66	0.3	209	
11/17/78	996	141.9	1.30	5.08	0.6	206	5
11/17/78	953	141.3	0.99	5.08	0.5	157	6
11/17/78	718	150.6	2.15	5.07	0.3	339	4
11/18/78	953	183.3	3.77	3.84	0.4	463	
11/20/78	455	167.0	3.39	3.49	0.3	375	
11/28/78	3.3	202.6	4.16	4.25	0.7	575	
12/1/78	1.0	102.0	1.39	5.41	1.5	228	
12/4/78	978	190.5	10.2	1.88	2.7	597	
12/4/78	896	204.8	2.85	6.99	5.8	651	
12/5/78	937	243.8	2.79	7.73	1.1	724	5

TABLE 2 (cont)

Notes:

1. Receiver aperture covered and insulated.
2. Loss measured using 26.7 cm aperture. Unless noted all others are 30.5 aperture.
3. Loss measured using 20.3 cm aperture.
4. Collector elevation approximately 25^{o}.
5. Collector elevation approximately 45^{o}.
6. Collector elevation approximately 60^{o}.

$\sim 20\text{-}30^{o}$ elevation. For plotting in Figure 15, elevation angles below $\sim 45^{o}$ were called low angles, those above $\sim 45^{o}$ were plotted as high angles.

Table 2 contains thermal loss data obtained from both receivers. Figure 15 shows the thermal losses as measured from the redesigned receiver.

Figure 16 is a comparison of thermal losses, showing the significant reduction in loss resulting from a simple wind shield and a relatively small amount of added insulation.

The 26 meters of small-diameter absorber tubing inside the receiver required large pumping pressures to achieve fairly low fluid flow rates. Figure 17 illustrates the differential pressure required accross the original receiver at several temperatures. Both total pressure and pressure per meter length of absorber tubing are shown. Since the modifications to improve the receiver performance involved adding four additional coils of tubing, the required pumping pressures also increased slightly, as shown in Figure 18.

Therminol-66 is a reasonably thin fluid at operating temperatures--viscosity of T-66 is about 4 centipoise at $100^{o}C$[2], compared to about 0.3 centipoise for water. However, T-66 fluid viscosity increases exponentially below about $100^{o}C$, reaching about 50,000 centipoise at $-18^{o}C$. This factor caused some delays in cold morning startup of the GE EPC. The heat-transfer fluid internal to the main fluid loop was warmed above $100^{o}C$ prior to attempting circulation through the GE receiver. Even with maximum allowed pressures of about 690 kPa (100 psi) applied, it sometimes took up to an hour to force all the cold fluid from the collector supply lines to establish enough flow to allow the receiver to be placed in focus.

The parabolic dish reflector system had a concentrated light safety problem slightly more severe than encountered with most parabolic trough reflectors. The prototype could not be stowed at a high elevation angle during high winds; it had to be anchored with an auxiliary bracing bar at a low elevation angle. At a low elevation, there was no azimuth position available that did not produce areas of concentrated light near ground level at some time during each day. This caused melting of plastic insulation covers, etc.,located within 3-6 cm of the dish. This problem was solved for the test series by covering the dish when testing was not in progress. Also, an operational system would have a greater range of azimuth and elevation angles than was available on the prototype. However, in designing a field of parabolic dish collectors, the position selected for stowing nonoperating collectors must not produce unacceptable hazards in the surrounding area.

Another aspect of this problem is the concentrated light hazard to the eyes of operating and visiting personnel. All concentrating collectors produce areas of hazardous concentrated light, the parabolic dish just covers a wider area because of the relatively large size and the higher concentration ratios available. Also, when not in focus, and parked at a low elevation angle, the areas where concentrated light

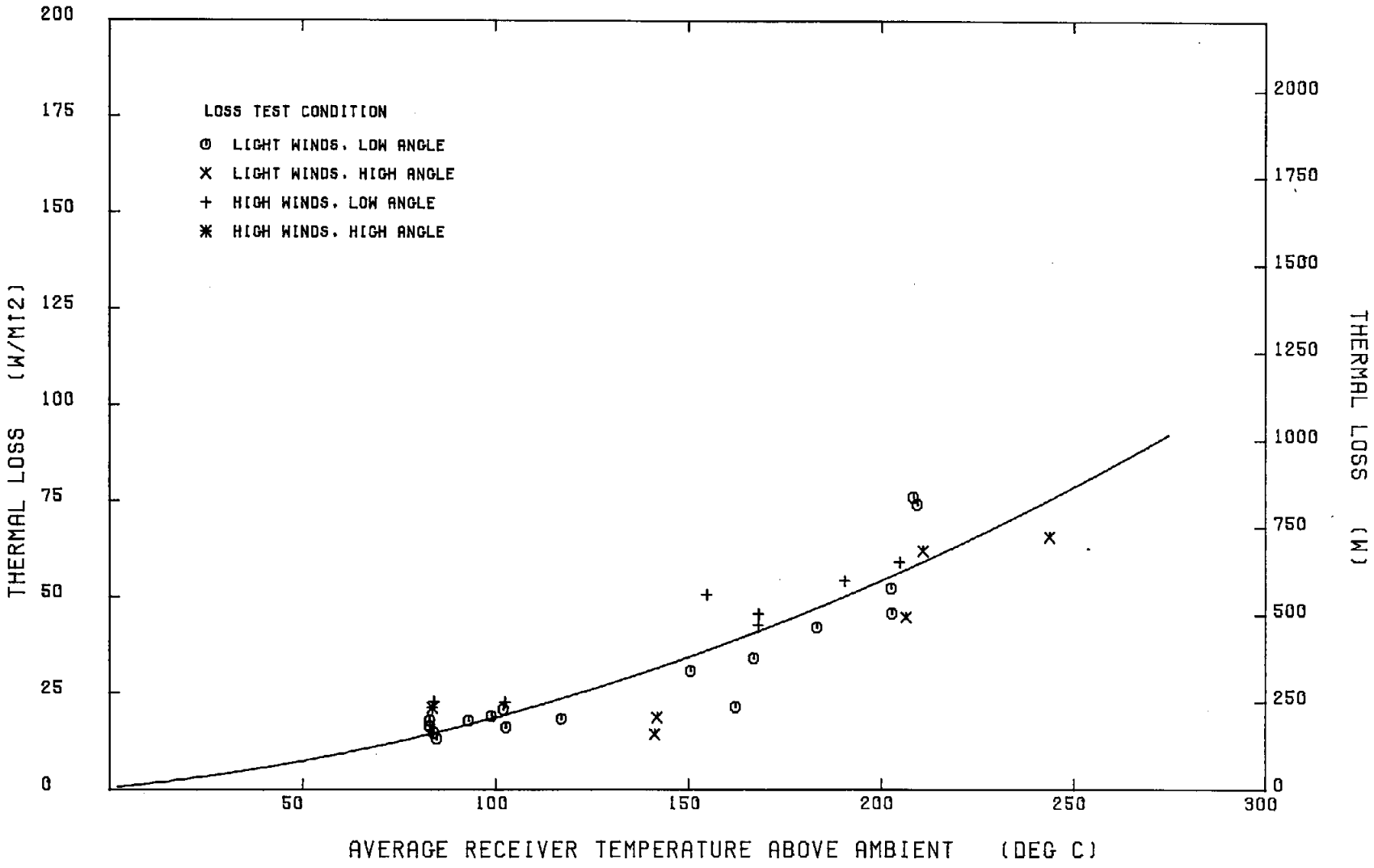

FIGURE 15 GE PARABOLIC DISH RECEIVER THERMAL LOSS (REDESIGNED RECEIVER)

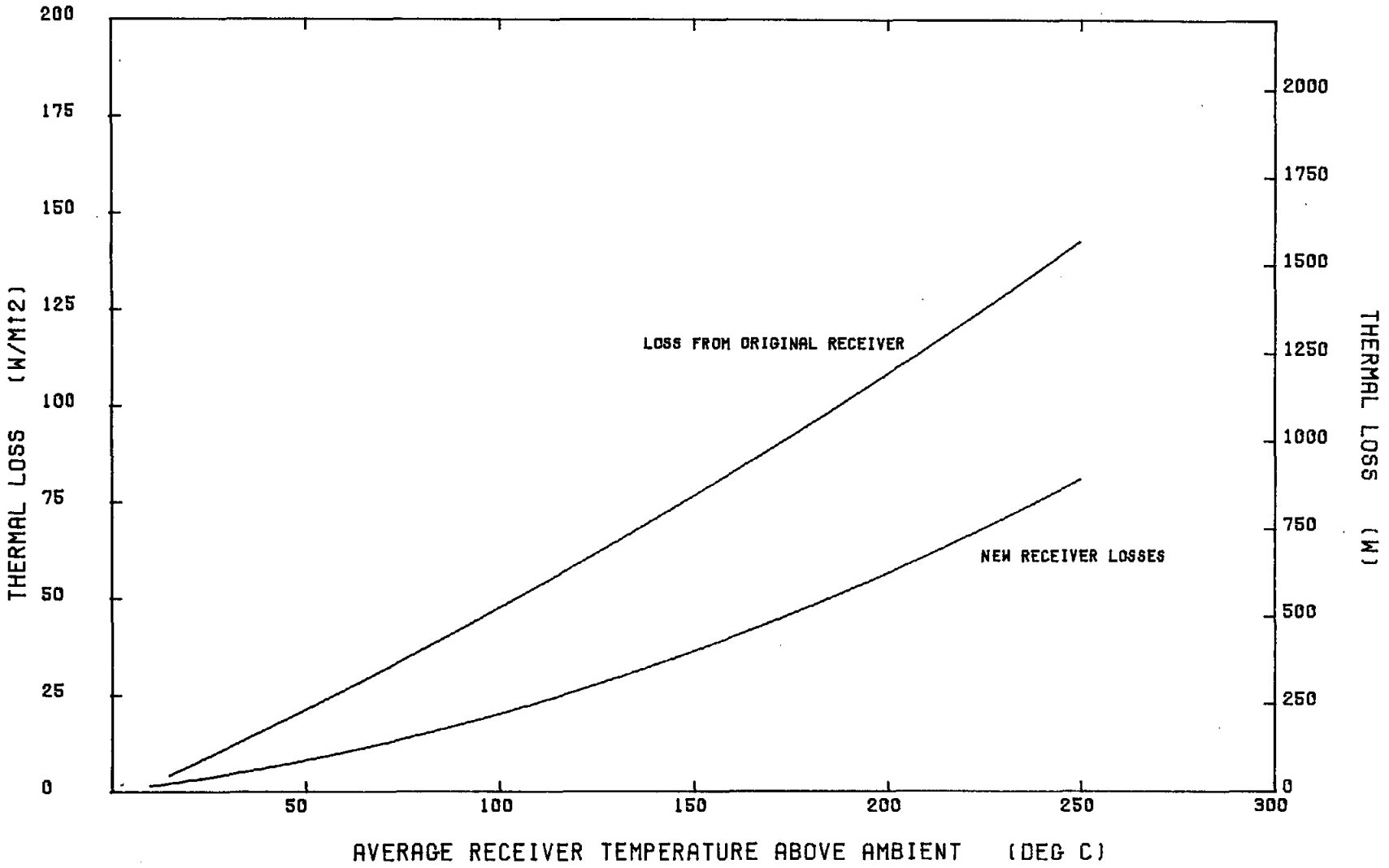

FIGURE 16 GE PARABOLIC DISH RECEIVER THERMAL LOSS COMPARISON

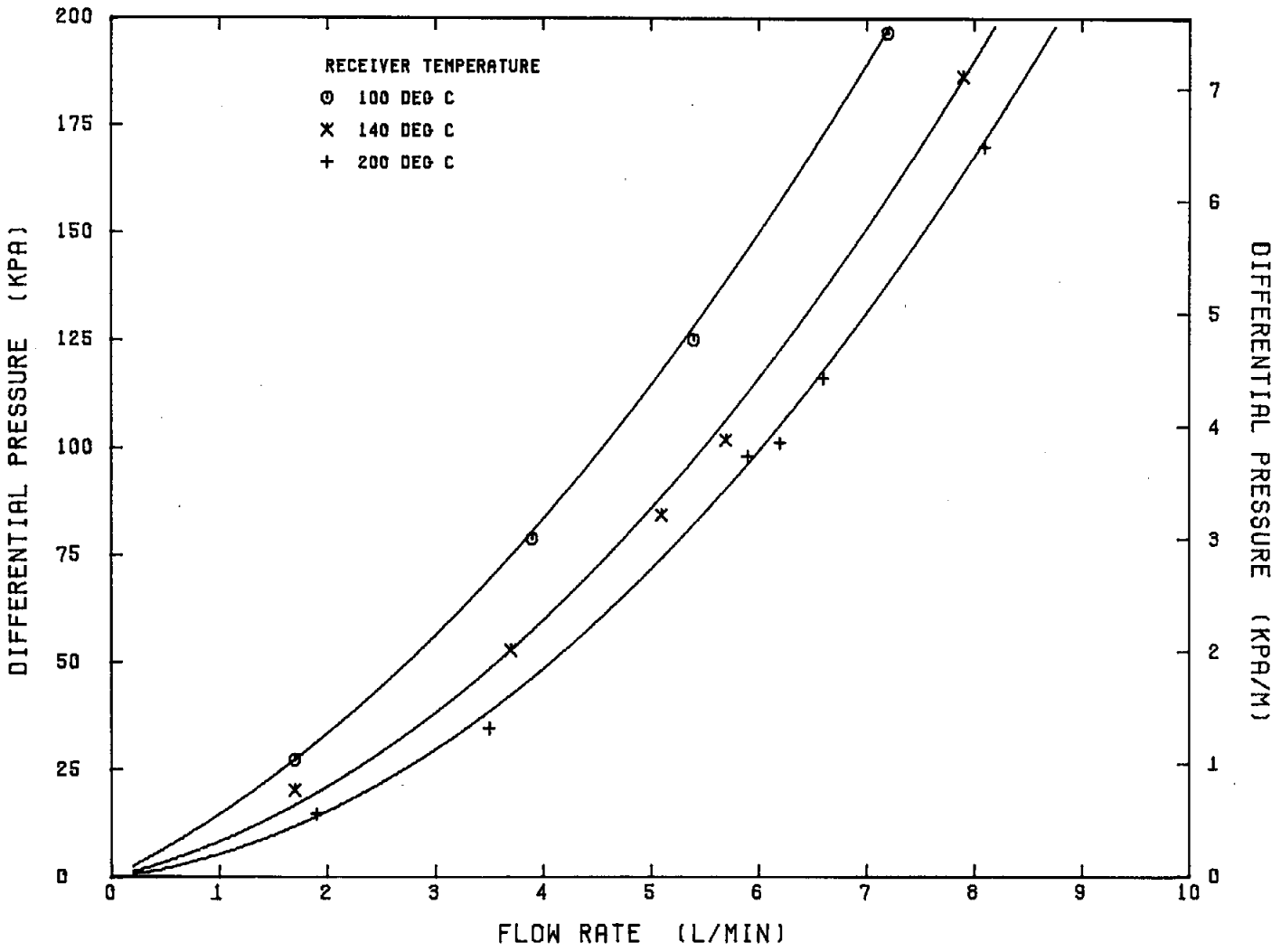

FIGURE 17. GE RECEIVER DIFFERENTIAL PRESSURE (ORIGINAL RECEIVER)

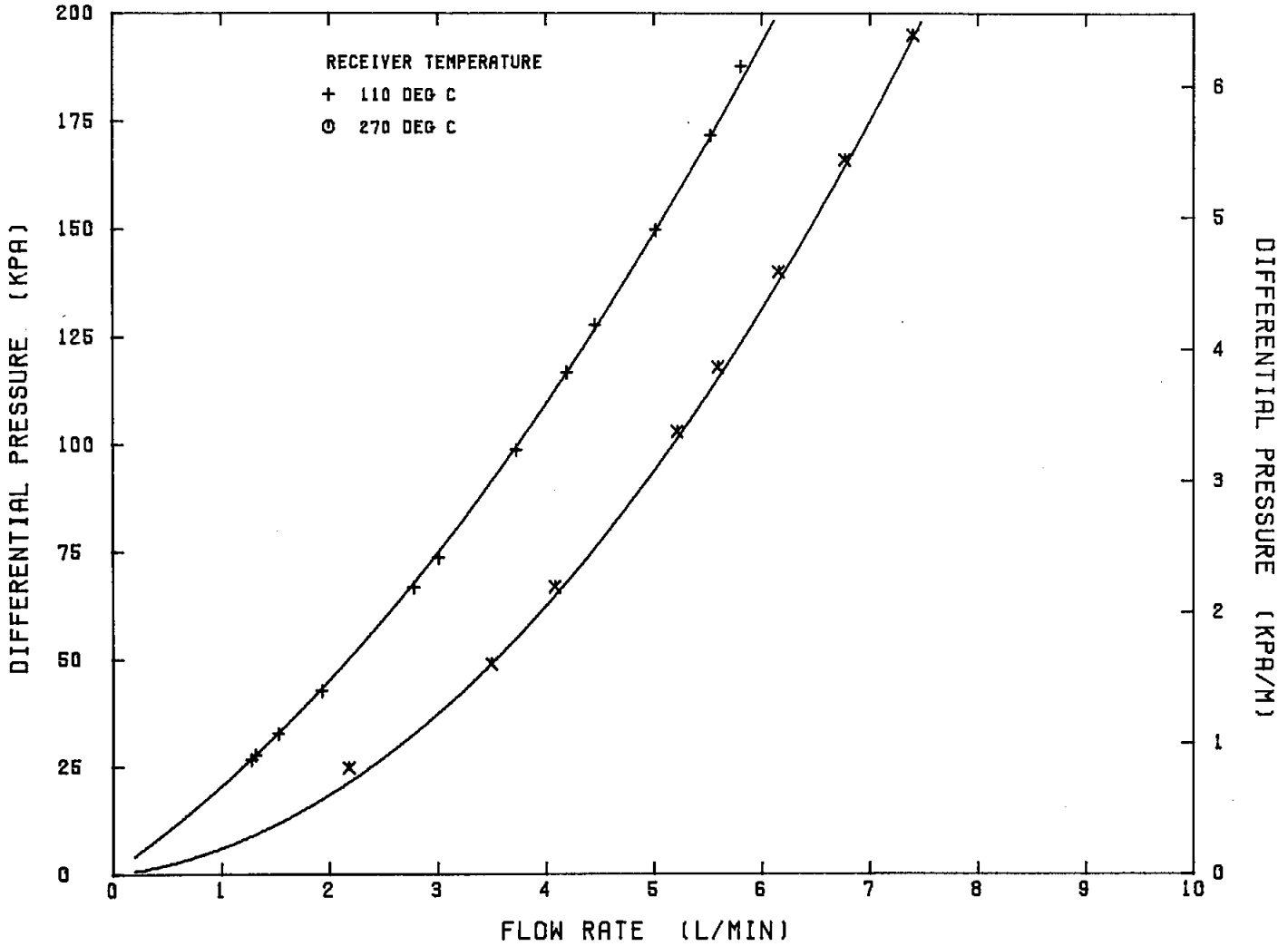

FIGURE 18. GE RECEIVER DIFFERENTIAL PRESSURE (REDESIGNED RECEIVER)

would be encountered were not always intuitively obvious to personnel working around the dish. They frequently walked into or through these areas before realizing concentrated light was there.

When in focus, the interior of the receiver was visible from the area near the dish. The light concentration was sufficiently high (up to ∿200 times normal sun intensity) that the light reflected from the receiver interior was made too bright to look at without protective glasses, a fact not always realized by visitors.

Summary of Results and Conclusions

Significant improvements were made in the performance of the GE EPC during the test cycle. Final efficiency performance ranged from about 60% at 100°C to about 53% at 300°C. A series of similar collectors are now being designed for test as a part of the Sandia/DOE MSSTF total energy system. Many of the design compromises accepted for the prototype test will be eliminated; further improvements in performance are expected.

The problems encountered with cold morning startup illustrate the necessity for designing an operational field of collectors so that large volumes of cold heat-transfer fluid do not have to be forced through long lengths of small diameter receiver tubing. Otherwise, the time required to establish a satisfactory flow rate may be unacceptably long.

The concentrated light levels found around the GE EPC confirm a rule that should apply to all concentrating collectors: the area around these devices should be strictly controlled, and access allowed only to knowledgeable and suitably protected personnel.

References

1. Solar Total Energy Program Plan, SAND76-0167, (Revised) Sandia Laboratories, Albuquerque, NM, August 1976.
2. Therminol 66, Technical Data Sheet, IC/FF-35, Monsanto Company.
3. Heiser, G., Test Plan, Engineering Prototype Collector, General Electric Company.

Distribution
TID-4500-R66,UC62(268)

Aerospace Corporation
101 Continental Blvd.
El Segundo, CA 90245
Attn: Elliott L. Katz

Acurex Aerotherm
485 Clyde Avenue
Mountain View, CA 94042
Attn: G. J. Neuner

Solar Total Energy Program
American Technological Univ.
P.O. Box 1416
Killeen, TX 76541
Attn: B. L. Hale

Argonne National Laboratory (3)
9700 South Cass Avenue
Argonne, IL 60439
Attn: R. G. Matlock
W. W. Schertz
Roland Winston

Atlantic Richfield Co.
515 South Flower Street
Los Angeles, CA 90071
Attn: H. R. Blieden

Baber Nichols Engineering
6325 W. 55th Avenue
Arvada, CO 80002
Attn: R. G. Olander

Battelle Memorial Institute
Pacific Northwest Laboratory
P.O. Box 999
Richland, WA 99352
Attn: K. Drumheller

Brookhaven National Laboratory
Associated Universities, Inc.
Upton, LI, NY 11973
Attn: J. Blewett

Congressional Research Service
Library of Congress
Washington, DC 20540
Attn: H. Bullis

Del Manufacturing Co.
905 Monterey Pass Road
Monterey Park, CA 91754
Attn: M. M. Delgado

Desert Research Institute
Energy Systems Laboratory
1500 Buchanan Blvd.
Boulder City, NV 89005
Attn: Jerry O. Bradley

DSET
Black Canyon Stage
P.O. Box 185
Phoenix, AZ 85029
Attn: Gene A. Zerlaut

Honorable Pete V. Domenici
Room 405
Russell Senate Office Bldg.
Washington, DC 20510

Edison Electric Institute
90 Park Avenue
New York, NY 10016
Attn: L. O. Elsaesser

Energy Institute
1700 Las Lomas
Albuquerque, NM 97131
Attn: T. T. Shishman

EPRI
3412 Hillview Avenue
Palo Alto, CA 94303
Attn: J. E. Bigger

General Atomic
P.O. Box 81608
San Diego, CA 92138
Attn: Alan Schwartz

General Electric Company
Valley Forge Space Center
Valley Forge, PA 19087
Attn: Walt Pijawka

General Electric Company
P.O. Box 8661
Philadelphia, PA 19101
Attn: A. J. Poche

Georgia Institute of Technology
School of Mechanical Engineering
Atlanta, GA 30332
Attn: S. Peter Kezios
President
American Society of
Mechanical Engineers

Georgia Institute of Technology
Atlanta, GA 30332
Attn: J. D. Walton

Georgia Power Company
Atlanta, GA 30302
Attn: Mr. Walter Hensley
Vice President
Economics Services

Gruman Corporation
4175 Veterans Memorial Highway
Ronkonkoma, NY 11779
Attn: Ed Diamond

Hexcel
11711 Dublin Blvd.
Dublin, CA 94566
Attn: George P. Branch

Industrial Energy Control Corp.
118 Broadway
Hillsdale, NJ 07675
Attn: Peter Groome

Jet Propulsion Laboratory
4800 Oak Grove Drive
Pasadena, CA 91103
Attn: V. C. Truscello

Kingston Industries Corp.
205 Lexington Avenue
New York, NY 10016
Attn: Ken Brandt

Lawrence Berkley Laboratory
University of California
Berkley, CA 94720
Attn: Mike Wallig

Lawrence Livermore Laboratory
University of California
P.O. Box 808
Livermore, CA 94500
Attn: W. C. Dickinson

Distribution (Cont)

Los Alamos Scientific Lab (3)
Los Alamos, NM 87545
Attn: J. D. Balcomb
C. D. Bankston
D. P. Grimmer

Honorable Manuel Lujan
1324 Longworth Building
Washington, DC 20515

Mann-Russell Electronics, Inc.
1401 Thorne Road
Tacoma, WA 98421
Attn: G. F. Russell

Martin Marietta Aerospace
P.O. Box 179
Denver, CO 80201
Attn: R. C. Rozycki

McDonnell Dogulas Astronautics Co.
5301 Bolsa Avenue
Huntington Beach, CA 92647
Attn: Don Steinmeyer

NASA-Lewis Research Center
Cleveland, OH 44135
Attn: R. Hyland

New Mexico State University
Solar Energy Department
Las Cruses, NM 88001

Oak Ridge Associated Universities
P.O. Box 117
Oak Ridge, TN 37830
Attn: A. Roy

Oak Ridge National Laboratory (4)
P.O. Box Y
Oak Ridge, TN 37830
Attn: J. R. Blevins
C. V. Chester
J. Johnson
S. I. Kaplan

Office of Technology Assessment
U. S. Congress
Washington, DC 20510
Attn: Dr. Henry Kelly

Omnium G (2)
1815 Orangethorpe Park
Anaheim, CA 92801
Attn: Ron Derby
S. P. Lazzara

PRC Energy Analysis Company
7600 Old Springhouse Road
McLean, VA 22102
Attn: K. T. Cherian

Rocket Research Company
York Center
Redmond, WA 98052
Attn: R. J. Stryer

Honorable Harold Runnels
1535 Longworth Building
Washington, DC 20515

Honorable Harrison H. Schmitt
Room 1251
Dirksen Senate Office Bldg.
Washington, DC 20510

Scientific Atlanta, Inc.
3845 Pleasantdale Road
Atlanta, GA 30340
Attn: Andrew L. Blackshaw

Sensor Technology, Inc.
21012 Lassen Street
Chatsworth, CA 91311
Attn: Irwin Rubin

Solar Energy Research Institute (7)
1536 Cole Blvd.
Golden, CO 80401
Attn: C. J. Bishop
Ken Brown
B. L. Butler
Frank Kreith
Charles Grosskreutz
B. P. Gupta
A. Rabl

Solar Energy Technology
Rocketdyne Division
6633 Canoga Avenue
Canoga Park, CA 91304
Attn: J. M. Friefeld

Solar Kinetics, Inc.
P.O. Box 10764
Dallas, TX 75207
Attn: Gus Hutchison

Southwest Research Institute
P.O. Box 28510
San Antonio, TX 78284
Attn: Danny M. Deffenbaugh

Stanford Research Institute
Menol Park, CA 94025
Attn: Arthur J. Slemmons

Stone & Webster
Box 5406
Denver, CO 80217
Attn: V. O. Staub

Sun Gas Company
Suite 800, 2 No. Pk. E
Dallas, TX 75231
Attn: R. C. Clark

Sundstrand Electric Power
4747 Harrison Avenue
Rockford, IL 61101
Attn: A. W. Adam

Sunsearch, Inc.
669 Boston Post Road,
Guilford, CT 06437
Attn: E. M. Barber, Jr.

Suntec Systems Inc.
2101 Wooddale Dr.
St. Paul, MN 55119
Attn: J. H. Davison

Swedlon, Inc.
12122 Western Avenue
Garden Grove, CA 92645
Attn: E. Nixon

TEAM Inc.
8136 Ola Keene Mill Road
Springfield, VA 22152

Distribution (Cont)

U. S. Department of Energy (2)
Agricultural & Industrial Process Heat
Conservation & Solar Application
Washington, DC 20545
Attn: W. W. Auer
J. Dollard

U. S. Department of Energy (3)
Albuquerque Operations Office
P.O. Box 5400
Albuquerque, NM 87185
Attn: K. K. Nowlin
G. Pappas
J. R. Roder

U. S. Department of Energy
Division of Energy Storage Systems
Washington, DC 20545
Attn: C. J. Swet

U. S. Department of Energy (9)
Division of Central Solar Technology
Washington, DC 20545
Attn: R. H. Annan
G. W. Braun
H. Coleman
M. U. Gutstein
G. M. Kaplan
Lou Melamed
J. E. Rannels
M. E. Resner
J. Weisiger

U. S. Department of Energy
Los Angeles Operations Office
350 S. Figueroa Street
Suite 285
Los Angeles, CA 90071
Attn: Fred A. Blaski

U. S. Department of Energy
San Francisco Operations Office
1333 Broadway, Wells Fargo Bldg.
Oakland, CA 94612
Attn: Jack Blasy

University of Delaware
Institute of Energy Conservation
Newark, DE 19711
Attn: K. W. Boer

Watt Engineering Ltd.
RR1, Box 183 1/2
Cedaredge, CO 81413
Attn: A. D. Watt

Western Control Systems
13640 Silver Lake Drive
Poway, CA 92064
Attn: L. P. Cappiello

Westinghouse Electric Corp.
P.O. Box 10864
Pittsburgh, PA 15236
Attn: J. Buggy

Centro de Fisica da Materia Condensada
Av. Prof. Gama Pinto, 2
1.699 Lisboa Codex
Portugal
Attn: Manuel Collares Pereira

1500 W. A. Gardner
1550 F. W. Neilson
2300 J. C. King
3161 J. E. Mitchell
3700 J. C. Strassell
4000 A. Narath
4531 J. H. Renken
4700 J. H. Scott
4710 G. E. Brandvold
4720 V. L. Dugan
4721 J. V. Otts (2/3)
4722 J. F. Banas
4723 W. P. Schimmel
4725 J. A. Leonard
4730 H. M. Stoller
5512 H. C. Hardee
5520 T. B. Lane
5600 D. B. Shuster
5834 D. M. Mattox
Attn: 5831 N. J. Magnani
5840 H. J. Saxton
Attn: 5810 R. G. Kepler
5820 R. L. Schwoebel
5830 M. J. Davis
5844 F. P. Gerstle
Attn: 5842 J. N. Sweet
5846 E. K. Beauchamp
8100 L. Gutierrez
8450 R. C. Wayne
8266 E. A. Aas
8470 C. S. Selvage
9572 L. G. Rainhart
9700 R. W. Hunnicutt
Attn: 9740 H. H. Pastorius
3141 T. L. Werner (5)
3151 W. L. Arner (3)
For DOE/TIC
(Unlimited Release)